Egypt. J. Chem. **Vol. 64**, No. 10, pp. 5663 - 5681 (2021)

Egyptian Journal of Chemistry

http://ejchem.journals.ekb.eg/

DFT, Electronic absorption spectra and Non-linear optical properties of some 4H-benzo[h]chromene Derivatives. Solvent effect and TD-DFT Approach

H. Moustafa[a]*, Abdelrahim. Z. Moussa[b], Mohamed E. Elshakre[a], Huwaida .M. E. Hassaneen[a]

[a]*Chemistry Department, College of Science, Cairo University, University Ave, Dokki, Giza, 12613, Egypt*
[b]*Institute of Graduate Studies and Environmental Research, Damanhour University, Beheira, 22762,Egypt*

Abstract

The electronic structure of some **4H-benzo[h]chromene** derivatives are investigated theoretically at the B3LYP/6-311++G (d,p) level of theory. The extent of delocalization and intramolecular charge transfer are estimated and discussed in terms of natural bond orbital analysis (NBO) and second order perturbation interactions between donor and acceptor MOs. The calculated E_{HOMO} and E_{LUMO} energies of the studied compounds can be used to calculate the global properties; chemical hardness (η), softness (S) and electronegativity (χ). The equilibrium geometries of the studied compounds are determined, and it was found that these geometries are non-planar. The calculated nonlinear optical parameters (NLO); polarizability (α), anisotropy of the polarizibility (Δα) and first order hyperpolarizibility (β) of the studied compounds show promising optical properties. The molecular electrostatic potential (MEP) and Local reactivity descriptors (fukui function) have been studied for the title compound and its derivatives at the same level of theory. Electronic spectra of 4H-benzo[h]chromene derivatives in different organic solvents such as 1,4-Dioxane and DiChloroEthane as non-polar solvents and Ethanol, Methanol and Acetonitrile as polar solvents, are investigated experimentally and theoretically using the time dependent density functional theory (TD-DFT) method at the B3LYP/6-311++G(d,p) level of the theory. The origin of the spectrum of the parent compound is found to be an additive one. The solvent effect is investigated experimentally and theoretically and a blue shift is discerned.

Keywords: B3LYP/6-311++G(d,p); 4H-benzo[h]chromene derivatives; NBO analysis; solvent effect; TD-DFT; UV.

1.Introduction

Chromenes (benzochromenes) are important heterocyclic compounds and generated great attention because of their interesting biological and pharmacological activities such as antioxidant[1–3], antiviral[4–6], antimicrobial[7,8], antifungal[9,10], antibacterial[11], antimalarial[12], anticancer[13–17], HIV-integrase inhibitory[18], anti-tubercular[19,20], TNF-a inhibitor[21], anti-toxoplasma[22], hypotensive[23]. Some of chromenes derivatives could also be used as inhibitors[24,25], mutagenicity[26], sex pheromone[27], in the treatment of Alzheimer's disease[28], Schizophrenia disorder[29] and anticancer agents through the inhibition of the c-Src Kinase enzyme[30]. Beside, chromenes have applications in various other fields; for example, they are employed as pigments[31], cosmetics, agrochemicals[32], laser dyes[33], optical brighteners[34] and fluorescence markers[35]. To the best of our knowledge there is a theoretical study for 2-amino-4H-chromene-3-carbonitrile (ACC), which compared with the experimental x-ray values[36], ACC compound is the main nucleus of the titled compound and its derivatives. Experimental data of compound 2-amino-4-(4-methoxyphenyl)-4H benzo[h]chromene-3-carbonitrile is available in the literature[37].

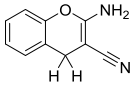

ACC

The X-ray data of 2-amino-4-(4-methoxyphenyl)-4H-benzo[h]chromene-3-carbonitrile is compared with

*Corresponding author e-mail: husseinmam@hotmail.com
Receive Date: 30 March 2021, Revise Date: 12 May 2021, Accept Date: 23 May 2021
DOI: 10.21608/EJCHEM.2021.69996.3544

the titled compound and its derivatives, theoretical calculation were carried out by density functional theory (B3LYP) using 6-311++G(d,p) as basis set . Density Functional Theory (DFT) based on the electronic density. DFT calculations include at least approximately the correlation energy. This technique has gained a considerable ground in recent years to become one of the most widely used techniques for the calculation of the ground state electronic energy. Its advantages include less demanding computational effort, i.e. less computer time, and in some cases better agreement with experimental values than the one obtained from other ab- initio procedures [38]. In recent years, theoretical, biological and spectroscopic studies of some pyrazol complexes, phosphorus Schiff base of some phosphinic acid and paraformaldehyde and some complexes of naphthalene-2-ol ligand. Different spectroscopic methods were used to characterize the ligands and its complexes. Different theoretical methods were used to optimize the ligand and complexes. The metal complexes exhibit marked biological activates against different bacteria.[39-41 Yet there is no systematic study of substituent and solvent effect on the observed spectra of the newly synthesized 2-amino-4-phenyl-4H-benzo[h]chromene-3-carbonitrile studied in this paper. So that, detailed knowledge on the structural and spectral behavior of 2-amino-4-phenyl-4H-benzo[h]chromene-3-carbonitrile is necessary prerequisite for understanding its chemical and biological properties. The main objective of our research is: to investigate the ground state geometrical parameters, effect of substituents of different electron donating-withdrawing power in the aryl moiety at position four. The electronic dipole moment (μ) , first order hyperpolarizibility(β) values and NBO analyses of the studied Chromenes derivatives have been computed, using B3LYP/6-311++G(d,p) to study the NLO properties and to provide valuable information about various intra- and intermolecular interactions. Global reactivity descriptors including electronegativity (χ), hardness (η), and softness (S) of the studied Chromenes derivatives were calculated and analyzed. Experimental and quantum chemical calculations of the electronic spectra of the Chromenes derivatives using time dependent density functional theory TD-DFT. The origin of each absorption band is identified and the contributing configurations and MOs are characterized. The theoretical and experimental UV spectra are obtained using 1,4-Dioxane and DichloroEthane as non-polar solvents and Ethanol, Methanol and Acetonitrile as polar solvents, respectively, to investigate the solvatochromic effect of the polarity of the different solvents on the absorption bands.

2. Experimental details

2.1. Synthesis

The titled compound and its derivatives were prepared according to published methods[42]. Reacting a mixture of different aromatic aldehydes, malononitrile and α-naphthol , under the same conditions, gave compound (1) 2-amino-4-phenyl-4H-benzo[h]chromene-3-carbonitrile, compound (2) 2-amino-4-(4-chlorophenyl)-4H-benzo[h]chromene-3-carbonitrile , compound (3) 2-amino-4-(4-methoxyphenyl)-4H-benzo[h]chromene-3-carbonitrile and compound (4) 2-amino-4-(4-nitrophenyl)-4H-benzo[h]chromene-3-carbonitrile as shown in scheme [1].

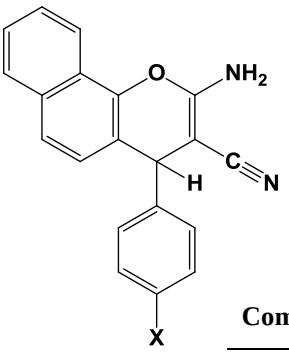

Compound	X
1	H
2	Cl
3	OCH_3
4	NO_2

Scheme [1].

2.2. Solvents and apparatus

UV-Vis spectrum of the titled compound and its derivatives spectra were recorded using a Perkin Elmer Lambda 4B spectrophotometer using 1.0 cm fused quartz cells, where the spectrometer records

linearly the percent of transmittance over the range 200–700 nm at room temperature using 1,4-Dioxane and Dichloroethane as non-polar solvents and Ethanol, Methanol and Acetonitrile as polar solvents.

2.3. Computational procedure

In this study, for meeting the requirements of both accuracy and time saving, theoretical methods and basis sets should be considered. DFT (B3LYP) method was used. DFT computations were performed by using Gaussian 09W[43] program which is a combination with the Becke's three parameter (local, non-local, and Hartree-Fock) hybrid exchange functional with Lee–Yang–Parr correlation functional (B3LYP)[44–46]. Full geometry optimization was performed using 6-311++G(d,p) as a basis set to generate the optimized structures and ground sate properties of the studied compounds, the stability of the optimized geometry was confirmed by frequency calculations which gave positive values for all the obtained wavenumbers, the geometric structure as well as parameters were obtained from Gauss view 5.0 program, The basis set 6-311++G(d, p) augmented by 'd' polarization functions on heavy atoms and 'p' polarization functions on hydrogen atoms as well as diffuse functions for both hydrogen and heavy atoms were used[47]. In order to understand the electronic properties, the theoretical UV-Visible spectra have been computed by TD-DFT method with 6-311++G(d, p) basis sets for gas phase and solvents (polar and non-polar) effect also have been taken into consideration by implementing Polarizable Continuum Model (PCM) . Also the non-linear optical properties were computed at the optimized geometry with the same level of theory. In addition, natural bond orbital (NBO) analysis was performed at the B3LYP/ 6-311G(d,p) level of theory.

3.Results and Discussion

3.1. Ground state geometric parameters

The optimized molecular structure of the tilted compound and its derivatives with atomic numbering and the vector of the dipole moment using DFT/B3LYP method with 6-311++G(d, p) as a basis set are indicated in (Fig. 1).

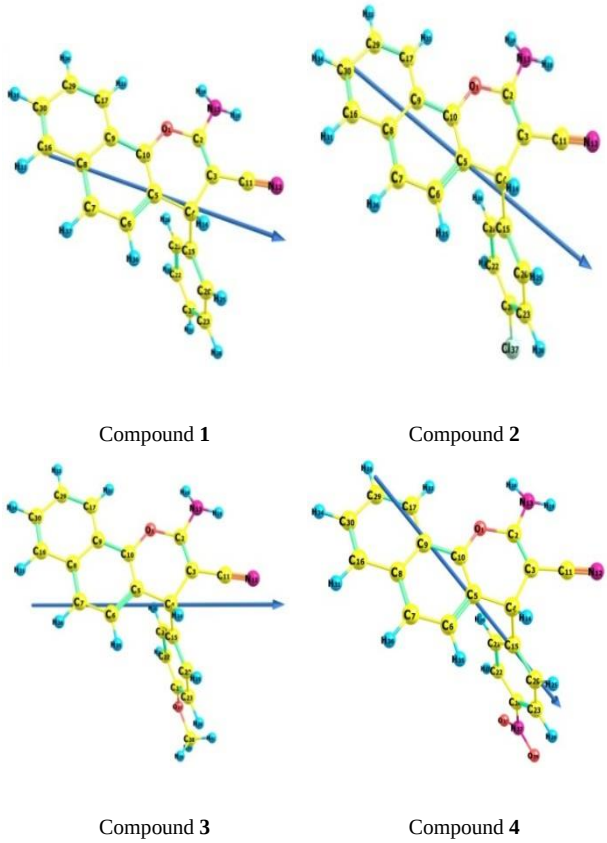

Fig. 1. Optimized geometry, the vector of the dipole moment and numbering system of the studied compounds (**1-4**) using B3LYP/6-311++G(d,p).

The selected bond lengths, bond angles and dihedral angles for the studied compounds **1-4** were listed together with corresponding selected X-ray experimental values as shown in (Table 1). The optimized bond lengths and bond angles are slightly difference from the experimental X-ray values, due to the fact that the experimental results belongs to molecule in solid states, while the theoretical calculation belongs to isolated molecule in gas phase. The fused 4H-benzo[h]chromene nuclei is almost planer with dihedral angles C_4-C_5-C_{10}-C_9= 179.27º and O_1-C_{10}-C_9-C_{17}=0.5º but the terminal phenyl ring is out of plane with dihedral angles C_3-C_4-C_{15}-C_{20} = 111.37º and C_3-C_4-C_{15}-C_{21} = 67.99º. The geometry of the studied compounds **1-4** don't change by insertion of Cl, OCH_3 and NO_2 groups in para-position of the terminal phenyl group as shown in (Fig. 1).

Table 1:Optimized geometrical parameters in bond lengths (Å), bond angles (0) and dihedral angles (0) of Compounds (**1**-**4**) calculated at B3LYP/6 311++G(d,p) level.

Compound **1**		Compound **2**		Compound **3**		Compound **4**		Experimental[a]
Bond lengths(Å)								
O_1-C_2	1.355	O_1-C_2	1.354	O_1-C_2	1.355	O_1-C_2	1.354	1.359
O_1-C_{10}	1.390	O_1-C_{10}	1.390	O_1-C_{10}	1.390	O_1-C_{10}	1.390	1.387
C_2-C_3	1.361	C_2-C_3	1.361	C_2-C_3	1.361	C_2-C_3	1.363	1.359
C_2-N_{13}	1.365	C_2-N_{13}	1.364	C_2-N_{13}	1.366	C_2-N_{13}	1.362	1.339
C_3-C_4	1.521	C_3-C_4	1.521	C_3-C_4	1.522	C_3-C_4	1.521	1.513
C_3-C_{11}	1.413	C_3-C_{11}	1.413	C_3-C_{11}	1.413	C_3-C_{11}	1.413	1.417
C_4-C_5	1.519	C_4-C_5	1.519	C_4-C_5	1.519	C_4-C_5	1.517	1.516
C_4-H_{14}	1.097	C_4-H_{14}	1.097	C_4-H_{14}	1.097	C_4-H_{14}	1.096	1.000
C_4-C_{15}	1.532	C_4-C_{15}	1.532	C_4-C_{15}	1.530	C_4-C_{15}	1.532	1.522
C_5-C_{10}	1.372	C_5-C_{10}	1.373	C_5-C_{10}	1.373	C_5-C_{10}	1.373	1.365
C_8-C_9	1.428	C_8-C_9	1.428	C_8-C_9	1.428	C_8-C_9	1.428	1.409
C_9-C_{10}	1.424	C_9-C_{10}	1.424	C_9-C_{10}	1.424	C_9-C_{10}	1.424	1.422
C_{11}-N_{12}	1.160	C_{11}-N_{12}	1.160	C_{11}-N_{12}	1.160	C_{11}-N_{12}	1.160	1.154
C_{15}-C_{20}	1.396	C_{15}-C_{20}	1.395	C_{15}-C_{20}	1.391	C_{15}-C_{20}	1.398	1.396
C_{20}-C_{23}	1.396	C_{20}-C_{23}	1.395	C_{20}-C_{23}	1.398	C_{20}-C_{23}	1.392	1.380
C_{23}-C_{24}	1.392	C_{23}-C_{24}	1.389	C_{23}-C_{24}	1.395	C_{23}-C_{24}	1.389	1.386
Bond angles(^{0})								
C_2-O_1-C_{10}	119.14	C_2-O_1-C_{10}	119.16	C_2-O_1-C_{10}	119.11	C_2-O_1-C_{10}	119.18	119.06
O_1-C_2-C_3	123.18	O_1-C_2-C_3	123.12	O_1-C_2-C_3	123.12	O_1-C_2-C_3	123.08	122.10
O_1-C_2-N_{13}	110.65	O_1-C_2-N_{13}	110.72	O_1-C_2-N_{13}	110.65	O_1-C_2-N_{13}	110.83	110.53
C_3-C_2-N_{13}	126.14	C_3-C_2-N_{13}	126.13	C_3-C_2-N_{13}	126.20	C_3-C_2-N_{13}	126.06	127.40
C_2-C_3-C_{11}	118.03	C_2-C_3-C_{11}	118.17	C_2-C_3-C_{11}	118.12	C_2-C_3-C_{11}	118.33	119.10
C_5-C_4-C_{15}	112.11	C_5-C_4-C_{15}	112.14	C_5-C_4-C_{15}	112.19	C_5-C_4-C_{15}	112.31	111.76
C_4-C_5-C_6	120.04	C_4-C_5-C_6	120.12	C_4-C_5-C_6	120.13	C_4-C_5-C_6	120.10	120.39
C_7-C_8-C_{16}	122.24	C_7-C_8-C_{16}	122.24	C_7-C_8-C_{16}	122.27	C_7-C_8-C_{16}	122.19	121.80
C_{10}-C_9-C_{17}	122.96	C_{10}-C_9-C_{17}	122.95	C_{10}-C_9-C_{17}	122.96	C_{10}-C_9-C_{17}	122.97	122.60
C_1-C_{10}-C_9	114.80	C_1-C_{10}-C_9	114.82	C_1-C_{10}-C_9	114.81	C_1-C_{10}-C_9	114.90	114.30
C_{20}-C_{15}-C_{21}	118.74	C_{20}-C_{15}-C_{21}	118.47	C_{20}-C_{15}-C_{21}	118.00	C_{20}-C_{15}-C_{21}	118.92	117.40
Dihedral angles(^{0})								
O_1-C_{10}-C_9-C_{17}	179.36	O_1-C_{10}-C_9-C_{17}	179.72	O_1-C_{10}-C_9-C_{17}	-179.91	O_1-C_{10}-C_9-C_{17}	179.83	179.20
C_4-C_3-C_2-N_{13}	-1.32	C_4-C_3-C_2-N_{13}	-1.19	C_4-C_3-C_2-N_{13}	-1.33	C_4-C_3-C_2-N_{13}	-0.95	-4.00
C_3-C_4-C_{15}-C_{20}	111.37	C_3-C_4-C_{15}-C_{20}	110.02	C_3-C_4-C_{15}-C_{20}	110.46	C_3-C_4-C_{15}-C_{20}	105.95	104.9
C_3-C_4-C_{15}-C_{21}	-68.00	C_3-C_4-C_{15}-C_{21}	-69.13	C_3-C_4-C_{15}-C_{21}	-68.58	C_3-C_4-C_{15}-C_{21}	-72.70	-74.00
C_4-C_5-C_6-C_7	-179.15	C_4-C_5-C_6-C_7	-178.99	C_4-C_5-C_6-C_7	-178.68	C_4-C_5-C_6-C_7	-179.05	-176.10
C_6-C_7-C_8-C_{16}	179.63	C_6-C_7-C_8-C_{16}	179.64	C_6-C_7-C_8-C_{16}	179.51	C_6-C_7-C_8-C_{16}	179.71	175.3
N_{13}-C_2-C_3-C_{11}	0.45	N_{13}-C_2-C_3-C_{11}	0.40	N_{13}-C_2-C_3-C_{11}	0.51	N_{13}-C_2-C_3-C_{11}	0.36	2.90

[a]X-ray data of compound **3** from Ref. [37]

3.2. Global reactivity descriptors

Table 2. represent all the global parameters calculated from molecular parameters using Koopmans' theorem and Kohn–Sham formalism [48, 49]. The results of calculation are helpful in predicting the correlation between the chemical parameters and activity of the studied compounds. Ionization potential (I) of any molecule corresponds to E_{HOMO} whereas E_{LUMO} corresponds to electron affinity value (A). Frontier orbital, HOMO and LUMO are very important to evaluate the reactivity/stability of molecules further

E_{HOMO} and E_{LUMO} are associated with electron donating and electron accepting ability respectively. Higher values of E_{HOMO} specify the nucleophilicity and lower value of E_{LUMO} accounts for the electrophilicity of any scaffold [48]. From data in Table 2.

Table 2

Theoretical gas phase total energy, E_{HOMO} and E_{LUMO} values and global reactivity descriptors of compounds (**1-4**).

	Compound **1**	Compound **2**	Compound **3**	Compound **4**
E_T(a.u)	-955.5257699	-1415.148558	-1070.082331	-1160.089465
E_{HOMO} (a.u)	-0.2246	-0.2288	-0.2215	-0.2363
E_{LUMO} (a.u)	-0.0630	-0.0668	-0.0610	-0.1050
Energy band gap = $\|E_{HOMO} - E_{LUMO}\|$ Ev	4.3968	4.4069	4.3680	3.5734
Ionization potential ($I=-E_{HOMO}$)Ev	6.1103	6.2254	6.0273	6.4301
Electron affinity ($A=-E_{LUMO}$) eV	1.7135	1.8185	1.6594	2.8567
Electronegativity $\chi=(I+A)/2$ Ev	3.9119	4.0220	3.8433	4.6434
Chemical Hardness ($\eta=(I-A)/2$) eV	2.1984	2.2034	2.1840	1.7867
chemical potential $p= -\chi$ eV	-3.9119	-4.0220	-3.8433	-4.6434
Electrophilicity index $\omega=p^2/2\eta$ eV	3.4805	3.6707	3.3817	6.0337
Chemical softness ($S=1/2\eta$) eV	0.4549	0.4538	0.4579	0.5597
μ(debye)	4.7916	5.6144	3.8428	8.2927

Compound **3** and **1** have highest E_{HOMO} and lowest E_{LUMO}. According to these parameters, the chemical reactivity varies with the structural configuration of molecules. Donor-acceptor behavior of a chemical system can be easily analyzed by hardness (η) and softness (S). A large energy gap represents a hard molecule and a soft molecule has a small energy gap. Therefore, soft molecules will be more polarizable as compared to the hard molecules. From the theoretical calculations, it was found that compound **4** has the lowest hardness value (η = 1.7867 eV) or has the highest softness (S= 0.5597 eV) which indicates that it is the least hard molecule or the most soft molecule in reduced moieties. The escaping tendency of an electron is measured by its chemical potential P (eV) and it is also related to its electronegativity. As P increases, tendency of a molecule to lose an electron increases. Electronegativity (χ) represents the molecular ability to attract electrons, the (χ) values displayed in (Table II) shows that Compounds **3** and **1** has lower electronegativity value compared to all the molecules. The chemical hardness and chemical potential are main factors of the overall reactivity of the molecule and are the most fundamental descriptors of charge transfer during a chemical reaction. Global electrophilicity (ω) predicts the state of stabilization after the saturation of system by electrons from the external environment. These reactivity information shows if a molecule is capable of donating charge. A good, more reactive, nucleophile is characterized by a lower value of (ω), while higher values indicate the presence of a good electrophile. Our results indicate that, compound **3** (ω = 3.3817 eV) has lower value of (ω), so, it is the most likely to accept electrons, thus energetically stabilizing the molecule. However, compound **4** is a good electrophile with ω = 6.0337 eV.

3.3. Natural bond orbital (NBO) analysis

The natural bond orbital (NBO) analysis provides enormous information for inter- and intra- molecular interactions which are important to understand the chemical phenomena such as the hydrogen bonding and the conjugative interactions in the molecular system [50-55]. NBO analysis was performed for all the studied compounds **1-4** using B3LYP/6-311G (d, p) level of theory in order to elucidate the delocalization of electron density within the molecules. It is also used to derive information on the changes of charge densities in proton donor and acceptor, namely in the bonding and antibonding orbitals. Delocalization of electron density between occupied Lewis-type (bond or lone pair) NBO orbitals and formally unoccupied (anti-bond or Rydberg) non-Lewis NBO orbitals correspond to a stabilizing donor-acceptor interaction. The energy E(2) which signifies the stabilization energy related

with i(donor)-j(acceptor) delocalization is estimated from the second order perturbation method. The higher value of stabilization energy E(2) shows the more intense is the interaction between electron donors and acceptors, that means the greater donating tendency from electron donors to acceptors NBO and the greater extent of conjugation of the complete system. The E(2) value calculated using

$$E^{(2)} = E_{ij} = \frac{q_i F(i,j)^2}{(\varepsilon_j - \varepsilon_i)} \quad (1)$$

Where q_i is the donor orbital occupancy, ε_i and ε_j are the diagonal elements and F (i,j) is the off-diagonal NBO Fock matrix element. The intensive electron donor- electron acceptor interaction, gives a high stabilization energy value of the $E^{(2)}$ (kJ mol^{-1}). The selected intensive interactions and perturbation energies are given in (Table 3).

In compound **1**, the selected resonance interaction energies for the donor-acceptor excitations of the π bonding orbitals or LP (lone pairs) to π* antibonding orbitals are π (C_2–C_3) → π*(C_{11}–N_{12}) 24.20 KJ mol^{-1}, LP_2 (O_1) → π*(C_2 – C_3) 32.15 KJ mol^{-1} and LP_1 (N_{13}) → π*(C_2–C_3) 41.64 KJ mol^{-1}. For compound **2** the resonance interaction energies for the donor-acceptor excitations are π (C_2–C_3) →π*(C_{11}–N_{12}) 24.26 KJ mol^{-1}, LP_2 (O_1) →π*(C_2–C_3) 32.21 KJ mol^{-1}, LP_1 (N_{13}) →π*(C_2–C_3) 42.59 KJ mol^{-1} and LP_3 (Cl_{37}) →π*(C_{23}–C_{24}) 12.31 KJ mol^{-1}. For compound **3** the resonance interaction energies for the donor-acceptor excitations are π (C_2 – C_3) →π* (C_{11} – N_{12}) 24.21 KJ mol^{-1}, LP_2 (O_1) →π* (C_2 – C_3) 31.98 KJ mol^{-1}, LP_1 (N_{13}) →π* (C_2 – C_3)41.15 KJ mol^{-1} and LP_2 (O_{37}) → π* (C_{23} – C_{24}) 30.57 KJ mol^{-1}. For compound **4** the resonance interaction energies for the donor-acceptor excitations are π (C_2 – C_3) → π* (C_{11} – N_{12}) 24.44 KJ mol^{-1}, LP_2 (O_1) → π* (C_2 –C_3) 32.38 KJ mol^{-1}, LP_1 (N_{13}) →π*(C_2 – C_3) 44.36 KJ mol^{-1}, LP_3 (O_{38}) → π* (N_{37} –O_{39}) 164.96 KJ mol^{-1} and LP_2 (O_{39}) →σ* (N_{37} – O_{38}) 18.71 KJ mol^{-1}. In all the studied compounds, the donor and acceptor orbitals played principal role in stabilizing the studied molecules. The charge transfer interaction has been formed by the orbital overlap between bonding and antibonding orbital which result in intramolecular charge transfer causing stabilization system. The types of charge transfer in the studied molecules are found to be n→σ∗, n→π∗ and π→π∗.

Table 3

Some selected second order perturbation interaction energy, E(2), population involved in the transition of the studied compounds (**1**–**4**) using the NBO at B3LYP/6-311G (d,p).

Donor (i)	type	occupancy	Acceptor (j)	type	occupancy	[a]E2 (KJ mol^{-1})	[b]E(j)-E(i) (a.u)	[c]F(i,j) (a.u)
Compound **1**								
C_2 - C_3	π	1.86073	C_{11} - N_{12}	π*	0.12254	24.20	0.40	0.088
C_8 - C_9	π	1.55434	C_5 - C_{10}	π*	0.31604	18.73	0.28	0.067
C_{15} - C_{20}	π	1.66584	C_{23} - C_{24}	π*	0.32266	20.56	0.28	0.068
C_{21} - C_{22}	π	1.67062	C_{15} - C_{20}	π*	0.34236	21.01	0.29	0.070
C_{23} - C_{24}	π	1.66912	C_{21} - C_{22}	π*	0.31456	20.25	0.29	0.068
O_1	LP(2)	1.80464	C_2 - C_3	π*	0.33457	32.15	0.37	0.101
N_{13}	LP(1)	1.79391	C_2 - C_3	π*	0.33457	41.64	0.32	0.106
Compound **2**								
C_2 - C_3	π	1.86010	C_{11} - N_{12}	π*	0.12266	24.26	0.40	0.089
C_8 - C_9	π	1.55415	C_5 - C_{10}	π*	0.31787	18.91	0.28	0.067
C_{15} - C_{20}	π	1.66133	C_{23} - C_{24}	π*	0.38243	21.84	0.27	0.069
C_{23} - C_{24}	π	1.68578	C_{21} - C_{22}	π*	0.30914	19.48	0.30	0.068
O_1	LP(2)	1.80433	C_2 - C_3	π*	0.33727	32.21	0.37	0.101
N_{13}	LP(1)	1.79059	C_2 - C_3	π*	0.33727	42.59	0.31	0.107
Cl_{37}	LP(3)	1.92893	C_{23} - C_{24}	π*	0.38243	12.31	0.33	0.062
Compound **3**								
C_2 - C_3	π	1.86094	C_{11} - N_{12}	π*	0.12288	24.21	0.40	0.088
C_{15} - C_{20}	π	1.69057	C_{21} - C_{22}	π*	0.30234	20.79	0.29	0.069
C_{21} - C_{22}	π	1.71161	C_{23} - C_{24}	π*	0.38160	21.66	0.28	0.071
C_{23} - C_{24}	π	1.66996	C_{15} - C_{20}	π*	0.34569	21.56	0.30	0.072

O_1	LP(2)	1.80478	C_2 - C_3	π*	0.33340	31.98	0.37	0.101
N_{13}	LP(1)	1.79570	C_2 - C_3	π*	0.33340	41.15	0.32	0.106
O_{37}	LP(2)	1.84079	C_{23} - C_{24}	π*	0.38160	30.57	0.34	0.097
Compound **4**								
C_2 - C_3	π	1.85799	C_{11} - N_{12}	π*	0.12338	24.44	0.40	0.089
C_{15} - C_{20}	π	1.63625	C_{23} - C_{24}	π*	0.36974	23.97	0.28	0.073
C_{21} - C_{22}	π	1.65598	C_{15} - C_{20}	π*	0.32715	21.97	0.29	0.072
O_1	LP(2)	1.80393	C_2 - C_3	π*	0.34188	32.38	0.37	0.102
N_{13}	LP(1)	1.78430	C_2 - C_3	π*	0.34188	44.36	0.31	0.108
O_{38}	LP(3)	1.44440	N_{37} - O_{39}	π*	0.62432	164.96	0.14	0.140
O_{39}	LP(2)	1.89847	N_{37} - O_{38}	σ*	0.05552	18.71	0.72	0.105

[a] E2 means energy of hyperconjucative interactions (stabilization energy).
[b] Energy difference between donor (i) and acceptor (j) NBO orbitals.
[c] F(i,j) is the Fock matrix element between i and j NBO orbital.

3.4. Fukui functions

Density Functional Theory is a powerful tool for the study of reactivity and selectivity in a molecule[46]. Fukui functions are indices that give information about the tendency of a molecule to lose or gain an electron thus predicting which atom in the molecule would be more prone to a nucleophilic or an electrophilic attack. When the molecule gains electrons (electron removal to the LUMO of the neutral molecule) it has reactivity site of the electrophilic attack f_j^- , when the molecule losses electrons (electron addition from the HOMO of the neutral molecule) it has reactivity site of the nucleophilic attack f_j^+ and when the molecule has neutral electrons then they are in radical attack f_j^0. Local electrophilicity (nucleophilic attack), Local nucleophilicity (electrophilic attack) and neutral (radical) attack properties of the studied compound and its derivatives on the corresponding condensed or atomic Fukui functions and given as

$$f_j^- = q_i(N) - q_i(N-1) \quad (2)$$

$$f_j^+ = q_i(N+1) - q_i(N) \quad (3)$$

In these equations, q_i is the atomic charge (evaluated from Mulliken population analysis, electrostatic derived charge, etc.) at the jth atomic site in the neutral (N), anionic (N + 1) or cationic (N - 1) chemical species. A dual descriptor (Δf(r)), which is defined as the difference between the nucleophilic and electrophilic Fukui function and is given by the equation,

$$\Delta f(r) = [f^+(r) - f^-(r)] \quad (4)$$

Table 4

The condensed Fukui functions (f_j^+), (f_j^-), (f_j^0) and dual descriptors Δf(r).

Compound **1**				Compound **2**				Compound **3**				Compound **4**			
Atoms	f_j^+	f_j^-	Δf(r)	Atoms	f_j^+	f_j^-	Δf(r)	Atoms	f_j^+	f_j^-	Δf(r)	Atoms	f_j^+	f_j^-	Δf(r)
O_1	0.004	0.082	-0.078	O_1	0.004	0.080	-0.076	O_1	0.004	0.060	-0.056	O_1	0.000	0.080	-0.080
C_2	0.030	0.066	-0.037	C_2	0.033	0.063	-0.030	C_2	0.029	0.069	-0.040	C_2	0.005	0.055	-0.050
C_3	0.023	0.271	-0.248	C_3	0.025	0.262	-0.237	C_3	0.024	0.235	-0.211	C_3	-0.001	0.245	-0.247
C_4	0.005	0.004	0.001	C_4	0.004	0.017	-0.013	C_4	0.004	0.021	-0.018	C_4	0.007	0.014	-0.006
C_5	0.077	0.084	-0.007	C_5	0.077	0.071	0.006	C_5	0.077	0.035	0.042	C_5	0.001	0.077	-0.076
C_6	0.060	0.023	0.036	C_6	0.055	0.029	0.026	C_6	0.062	0.020	0.041	C_6	0.001	0.034	-0.033
C_7	0.141	0.076	0.064	C_7	0.142	0.080	0.061	C_7	0.142	0.054	0.089	C_7	0.004	0.088	-0.084
C_8	0.006	0.002	0.004	C_8	0.007	0.003	0.004	C_8	0.007	0.004	0.003	C_8	0.001	0.003	-0.002

C_9	0.008	0.005	0.003	C_9	0.008	0.005	0.003	C_9	0.007	0.007	0.001	C_9	0.001	0.004	-0.003
C_{10}	0.130	0.066	0.064	C_{10}	0.131	0.062	0.069	C_{10}	0.128	0.024	0.105	C_{10}	0.005	0.071	-0.067
C_{11}	0.000	0.001	-0.001	C_{11}	-0.002	0.005	-0.007	C_{11}	-0.003	0.023	-0.026	C_{11}	0.006	0.003	0.003
N_{12}	0.011	0.096	-0.084	N_{12}	0.012	0.095	-0.083	N_{12}	0.011	0.085	-0.075	N_{12}	0.000	0.089	-0.089
N_{13}	0.011	0.061	-0.050	N_{13}	0.012	0.061	-0.049	N_{13}	0.011	0.074	-0.064	N_{13}	0.002	0.051	-0.049
C_{15}	0.008	-0.025	0.033	C_{15}	0.007	-0.008	0.015	C_{15}	0.004	0.046	-0.041	C_{15}	0.099	-0.008	0.107
C_{16}	0.145	0.036	0.108	C_{16}	0.139	0.039	0.100	C_{16}	0.149	0.020	0.130	C_{16}	0.001	0.048	-0.047
C_{17}	0.152	0.039	0.113	C_{17}	0.146	0.040	0.106	C_{17}	0.155	0.017	0.138	C_{17}	0.002	0.050	-0.048
C_{20}	0.025	-0.023	0.048	C_{20}	0.022	0.008	0.014	C_{20}	0.016	0.018	-0.002	C_{20}	0.009	0.005	0.004
C_{21}	-0.012	0.052	-0.064	C_{21}	-0.001	0.009	-0.009	C_{21}	-0.002	0.018	-0.020	C_{21}	0.011	0.012	-0.002
C_{22}	0.012	-0.006	0.018	C_{22}	0.014	-0.003	0.017	C_{22}	0.007	0.014	-0.007	C_{22}	0.087	-0.006	0.092
C_{23}	-0.004	0.011	-0.016	C_{23}	-0.003	0.007	-0.010	C_{23}	-0.001	0.031	-0.032	C_{23}	0.095	0.005	0.090
C_{24}	0.014	0.003	0.011	C_{24}	0.014	0.001	0.013	C_{24}	0.009	0.035	-0.026	C_{24}	0.028	0.000	0.028
C_{29}	0.074	0.021	0.053	C_{29}	0.071	0.023	0.048	C_{29}	0.076	0.015	0.061	C_{29}	0.001	0.027	-0.026
C_{30}	0.072	0.017	0.055	C_{30}	0.071	0.017	0.054	C_{30}	0.072	0.006	0.067	C_{30}	0.002	0.022	-0.020
				Cl_{37}	0.002	0.003	-0.001	O_{37}	0.001	0.038	-0.037	N_{37}	0.229	0.000	0.229
								C_{38}	0.000	0.000	-0.001	O_{38}	0.201	0.000	0.201
												O_{39}	0.201	0.001	0.200

If $\Delta f(r) > 0$, then the site is favored for a nucleophilic attack, where as if $\Delta f(r) < 0$, then the site may be favored for an electrophilic attack [56]. (Table 4) provides the complete details of Fukui function and dual descriptor values for selected atoms for the studied compounds and its derivatives. As a result (Table 4) of the calculations, it is obtained that C_{17},C_{16} and C_7 atoms is the most prone site to nucleophilic attack while C_3, N_{12} and O_1 atoms are the most prone sites to electrophilic attack for compound **1** and compound **2**, respectively and C_{17},C_{16} and C_{10} atoms are the most prone sites to nucleophilic attack while C_3, N_{12} and N_{13} atoms are the most prone sites to electrophilic attack for compound **3** and N_{37},O_{38} and O_{39} atoms is the most prone site to nucleophilic attack while C_3, N_{12} and C_7 atoms are the most prone sites to electrophilic attack for compound **4**.

3.5. Molecular electrostatic potential

The molecular electrostatic potential (MEP) is related to the electronic density and is a very useful descriptor for determining sites for nucleophilic and electrophilic reactions as well as hydrogen bonding interactions and chemical activity[57,58]. In the color scheme of MEPs, blue corresponds to electron deficient, partially positive charge which is preferred site for nucleophilic attack, red represents electron rich, partially negative charge which is the preferred site for electrophilic attack, yellow for slightly electron rich region; green for neutral respectively. The MEP maps were calculated at the B3LYP/6-311++G(d,p) level for the title compound and its derivative and demonstrated in (Fig. 2).

Negative regions are mainly over the CN group for the studied compounds (**1**-**4**) and the oxygen atoms of OCH_3 and NO_2 groups for compound **3** and **4** respectively. These are the most preferred regions for any electrophilic attack on the molecule. Besides, a maximum positive region is localized on N atom of NH_2 group for compounds (**1**-**4**), indicating a possible site for nucleophilic attack.

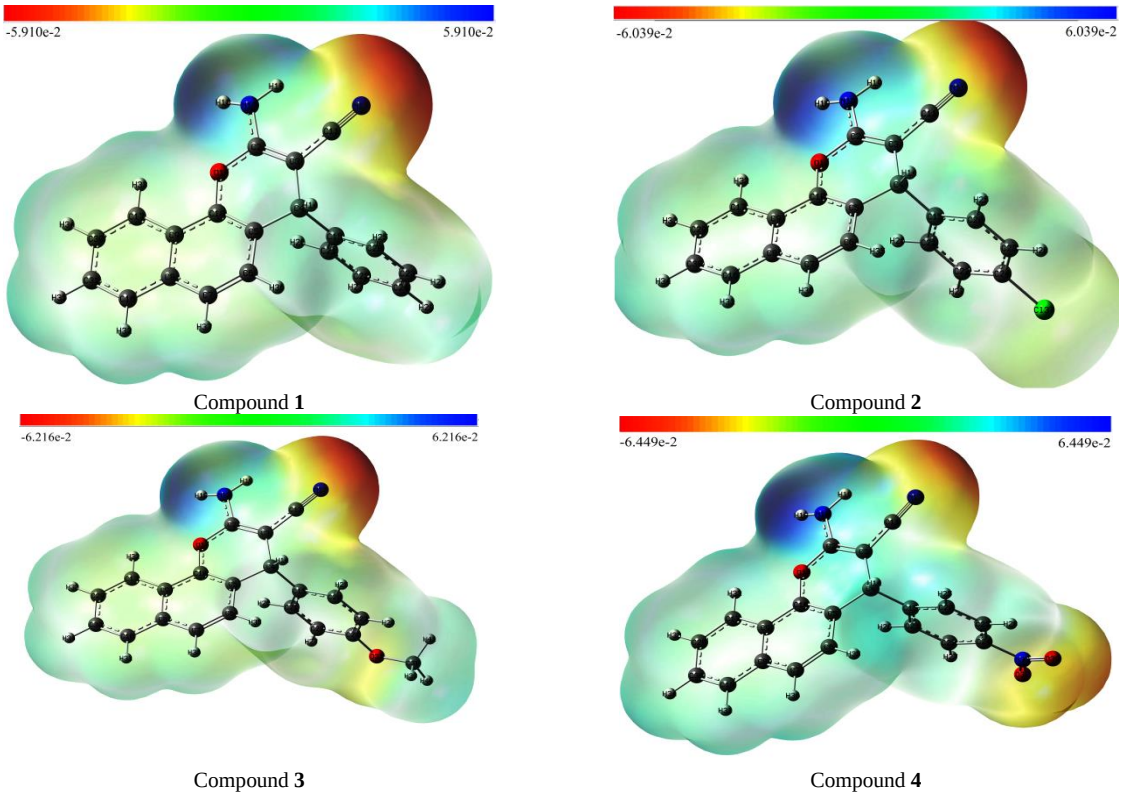

Fig. 2. Molecular Electrostatic Potential (MEP) surface diagram of compounds (**1-4**).

3.6. Non-linear optical properties (NLO)

In the recent years, compounds with non-linear optical properties are very important in modern communication technology, data storage and optical signal processing [59–61], Using the x, y and z components they are defined as [62,63]the polarizability (α) and hyperpolarizability (β) obtained from Gaussian 09 output are reported in atomic units (a.u.), the calculated values have been converted into electrostatic units (esu) (α: 1 a.u. = 0.1482 x10^{-24} esu; β: 1 a.u.= 8.6393 x10^{-33} esu) [64]. The ability of a compound to show this property can be obtained from polarizability and hyperpolarizability characterize the response of a system in an applied electric field and their values are given in (Table 5). At this point, the computational approach provides a non-expensive way for the determination of nonlinear optical properties, and thus, enables the prediction of potential use of the Chromene compounds as nonlinear optical materials. In this context, the NLO properties of the title compound and its derivatives were evaluated by the determining the polarizability (α) and the hyperpolarizability (β) using the following equations:

$$< \alpha >= \frac{\alpha_{xx}+\alpha_{yy}+\alpha_{zz}}{3} \quad (5)$$

$$\beta = \sqrt{(\beta_{xxx}+\beta_{xyy}+\beta_{xzz})^2 + (\beta_{yyy}+\beta_{yzz}+\beta_{yxx})^2 + (\beta_{zzz}+\beta_{zxx}+\beta_{zyy})^2} \quad (6)$$

The calculated values of polarizability (α) and the first hyperpolarizability (β) are 19.58x10^{-24} and 1.614 x 10^{-30} esu for compound **1**, 21.84x10^{-24} and 1.865 x 10^{-30} esu for compound **2**, 20.77x10^{-24} and 1.382 x 10^{-30} esu for compound **3** and 23.58x10^{-24} and 3.264 x 10^{-30} esu for compound **4** respectively. The β value of the title molecule and its derivatives are 12 (compound **1**), 14 (compound **2**), 10 (compound **3**) and 25 (compound **4**) greater than of the standard NLO material Urea (0.13 x 10^{-30} esu)[65] which is accepted as a prototype molecule for nonlinear optical materials[66,67]. Hence all the studied compounds (**1-4**) can be developed as possible materials with a potential to show non-linear optical activities.

Table 5

Calculated polarizability and 1st order hyperpolarizability components of compounds (1-4) with B3LYP/6-311++G (d, p) level of theory.

Compound	α_{xx}	α_{yy}	α_{zz}	α_{xy}	α_{xz}	α_{yz}	α_{TOT} au	α_{TOT} 10^{-23} esu
1	-138.350	-128.173	-129.902	14.595	-1.256	12.841	-132.142	-1.958
2	-150.937	-154.006	-137.234	-6.234	8.117	-15.054	-147.392	-2.184
3	-127.397	-152.073	-141.073	-14.871	8.707	-16.097	-140.181	-2.078
4	-175.357	-160.185	-141.901	5.492	14.045	-17.217	-159.148	-2.359

	β_{XXX}	β_{YYY}	β_{ZZZ}	β_{XYY}	β_{XXY}	β_{XXZ}	β_{XZZ}	β_{YZZ}	β_{YYZ}	β_{XYZ}	β_{TOT} au	β_{TOT} 10^{-30} esu
1	124.164	27.937	13.365	44.864	-91.134	29.446	-12.934	-1.436	36.966	-0.205	186.834	1.614
2	-107.355	-48.164	-14.685	-89.865	-40.014	-12.545	11.003	7.641	-46.628	6.198	215.912	1.865
3	80.361	-56.686	-13.757	-70.364	-94.203	-14.478	1.877	9.065	-44.846	2.160	159.988	1.382
4	-272.094	-67.337	-9.933	-101.423	32.803	6.997	-1.457	17.047	-40.426	-2.022	377.877	3.265

3.7. Absorption spectra and solvent effects

Electronic absorption spectroscopy of organic compounds are based on transition from n or π electrons to the π* excited state which normally take place in the UV-Vis region with wavelength from 200 nm to 800 nm. The experimental electronic spectra of the tilted compound and its derivatives were recorded in different organic solvents such as 1,4-Dioxane and DiChloroEthane as non-polar solvents and Ethanol, Methanol and Acetonitrile as polar solvents, and, Which have different dielectric constant (ε) 2.25 and 10.36 for non-polar solvents and 24.5, 32.7 and 37.5 for polar solvents respectively, whereas the calculated electronic absorption spectrum was obtained using time dependent-DFT (TD-DFT) calculations on the ground state optimized geometry of compounds (**1**-**4**), both in gas phase and solvent phase using IEFPCM model with different solvents, at the TD B3LYP/6-311++G(d,p) level of theory. The experimental absorbance of compounds (**1**-**4**) were found to be significant in the measured UV range (200-400 nm) and very low in the visible region (400-800 nm). Two possible types of interaction between subsystems can occur as shown in Scheme 2. For example, (i) no interaction between 2-amino-4H-benzo[h]chromene-3-carbonitrile and the terminal phenyl group Ph-X (ii) represent full conjugation between the two subsystems 2-amino-4H-benzo[h]chromene-3-carbonitrile and Ph-X.

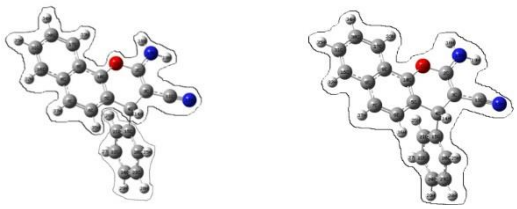

i ii

SCHEME 2. The two possible types of interaction between subsystems.

*3. 7. 1 Absorption spectra and solvent effects of compound **1**.*

The experimental absorption spectra of compound **1** are recorded in 1,4-Dioxane and DiChloroEthane as non-polar solvents and Ethanol, Methanol and Acetonitrile as polar solvents, the experimental and calculated UV-Vis spectra are shown in (Fig. 3) and the diagrams of some selected of HOMO and LUMO are indicated in (Fig. 4).

the most representative absorption wavelengths from experimental and calculation of compound **1** along

with the electronic transition configuration details involving the vertical excitation energy , the oscillator strengths (f) and major contribution are tabulated in (Table 6). In all solvents, compound **1** exhibited four bands; the first band has high intensity in all solvents, but the other three bands show very week and broad absorption bands in Ethanol, Methanol and Acetonitrile solvents and intermediate intensity and broad bands in DiChloroEthane, and 1,4-Dioxane. Increasing solvent polarity from1,4-Dioxane to Acetonitrile results in a blue shift of the first band only~ 17 nm but the other bands didn't affect by increasing solvent polarity. From (Table 6), we can conclude that the experimental and theoretical UV-Vis data are well agreed with each other.

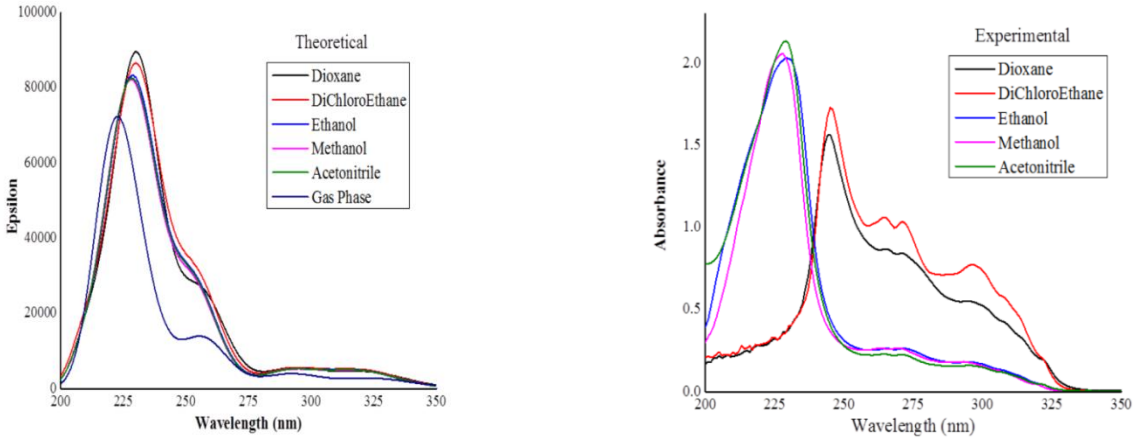

Fig. 3. Electronic absorption spectra of compound 1, experimental in dioxane, dichloroethane, ethanol, methanol and acetonitrile, theoretical in dioxane, dichloroethane, ethanol, methanol, acetonitrile and gas phase.

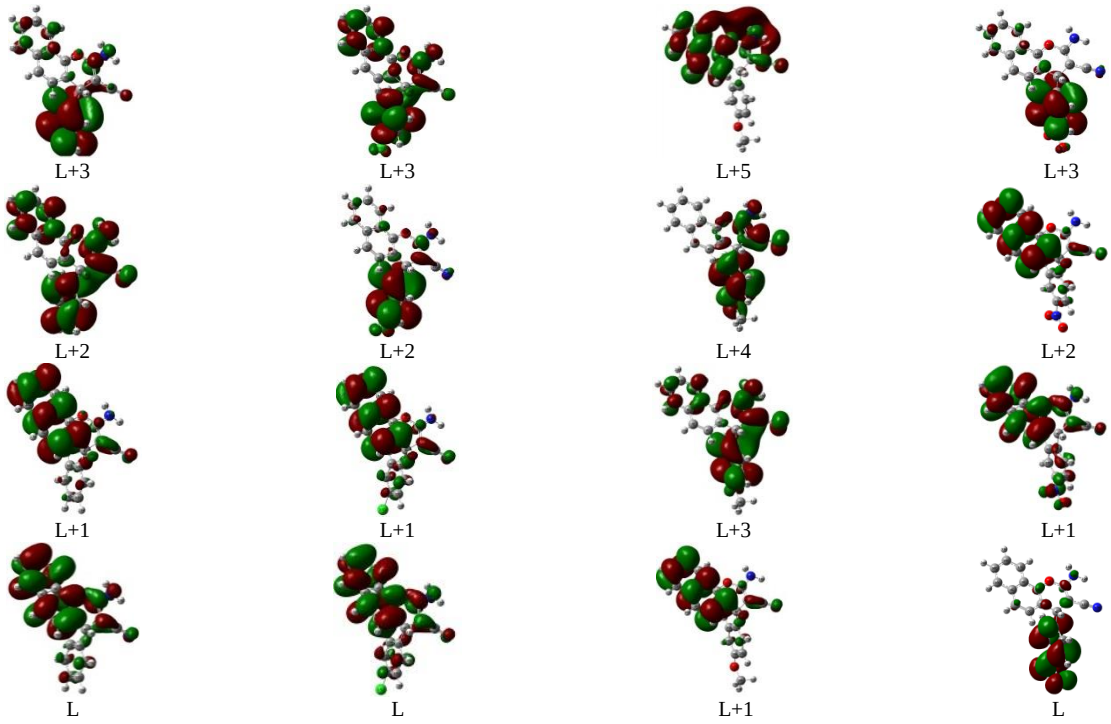

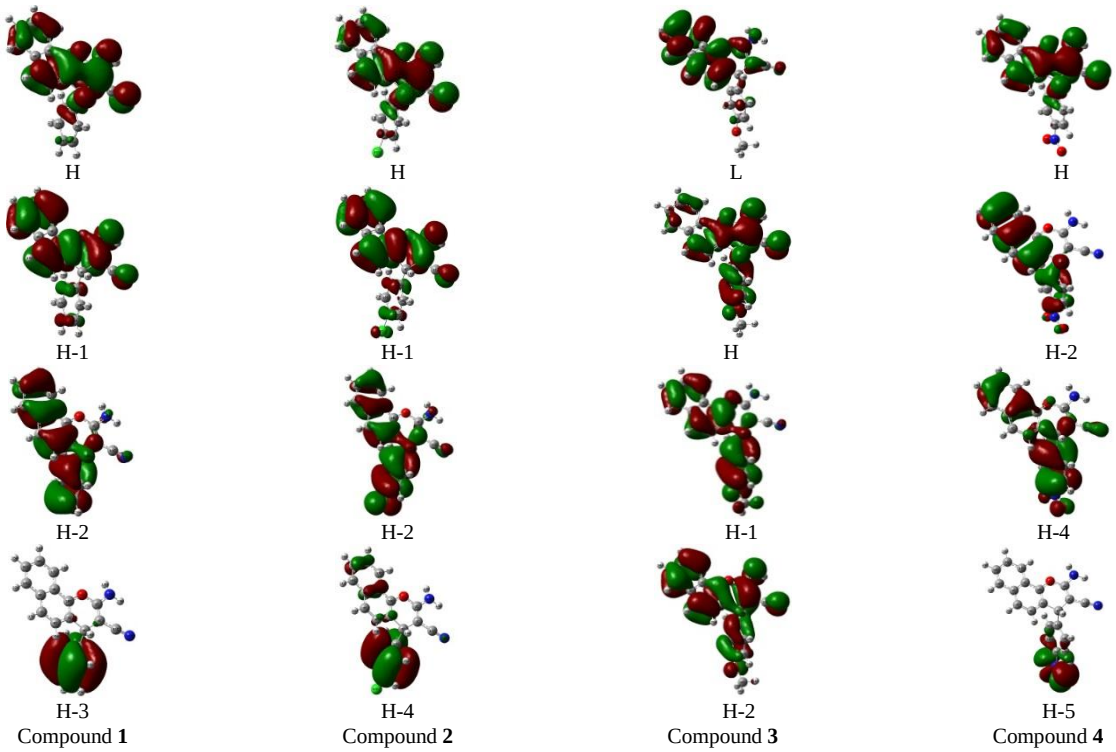

Fig. 4. Selected frontier molecular orbital (HOMO and LUMO) pictures for compounds (1-4), as obtained from DFT//B3LYP/6-31++G (d,p) level of calculation.

TABLE 6
Experimental and theoretical UV spectra of compound **1**, calculated at TD-B3LYP/6-311++G(d,p)

	Experimental		Theoretical			
	$\lambda_{max, nm}$	Abs	λ_{nm}	E(eV)	f	Major contribution
Gas phase	—	—	230	5.3934	0.1043	H-3->L+2 (14%), H-2->L+3 (28%)
	—	—	261	4.7456	0.0075	H->L+2 (82%)
	—	—	271	4.5623	0.0043	H-1->L+1 (40%), H->L+1 (44%)
	—	—	293	4.2309	0.0266	H-1->L+1 (58%), H->L+1 (20%)
1,4-Dioxane	245	1.562	244	5.0761	0.0357	H-1->L+2 (56%), H->L+5 (30%)
	265	0.868	260	4.7531	0.0101	H-1->L+1 (17%), H->L+2 (80%)
	271	0.843	269	4.6018	0.0087	H-2->L (18%), H-1->L+1 (36%)
	295	0.551	293	4.2319	0.0637	H-1->L (92%)
DiChloroEthane	245	1.730	245	5.0590	0.0305	H-1->L+2 (50%), H->L+4 (42%)
	265	1.061	261	4.7520	0.0115	H-1->L+1(23%), H->L+2(74%)
	271	1.034	268	4.6324	0.0061	H-1->L+1(33%), H->L+1 (38%)
	297	0.771	292	4.2463	0.0739	H-1->L (98%)
Ethanol	229	2.033	230	5.3827	0.2479	H-3->L+2 (18%), H-2->L+3 (23%), H-1->L+4 (17%)
	265	1.264	261	4.7510	0.0101	H-1->L+1 (24%), H->L+2 (73%)
	271	1.264	267	4.6385	0.0047	H-1->L+1(32%), H->L+1(37%)
	295	0.181	292	4.2513	0.0681	H-1->L (93%)
Methanol	228	2.057	227	5.4573	0.2794	H-2->L+1(19%), H-1->L+4(35%)
	264	0.266	261	4.7508	0.0096	H-1->L+1(24%), H-2->L (72%)
	269	0.266	267	4.6400	0.0044	H-1->L+1(32%), H->L+1(37%)

	293	0.183	292	4.2527	0.0643	H-1->L (88%)
Acetonitrile	229	2.134	230	5.3835	0.2411	H-3->L+2(18%), H-2->L+3 (23%), H-1->L+4(18%)
	264	0.229	261	4.7506	0.0098	H-1->L+1(24%), H->L+2(72%)
	271	0.227	267	4.6397	0.0045	H-1->L+1(32%), H->L+1(37%)
	295	0.160	292	4.2522	0.0654	H-1->L (88%)

*3. 7. 2. Absorption spectra and solvent effects of compound **2**.*

Compound **2** results by insertion of Cl atom in the Para position of 4-aryl of compound **1**. As in compound **1**, the experimental and theoretical electronic absorption spectra of compound **2** in 1,4-Dioxane and DiChloroEthane as non-polar solvents and Ethanol, Methanol and Acetonitrile as polar solvents are shown in (Fig. 5) and (Table 7). The charge density maps of some selected HOMO and LUMO are indicated in (Fig. 4). In all polar and non-polar solvents compound **2** exhibited four bands, the first band has high intensity in 1,4-Dioxane, DiChloroEthane and Methanol but broad band in Acetonitrile and Ethanol, but the other three bands show week and a broad bands in all solvents. The entire electronic absorption band for compound **2** and its major contributions are listed in Table 7.

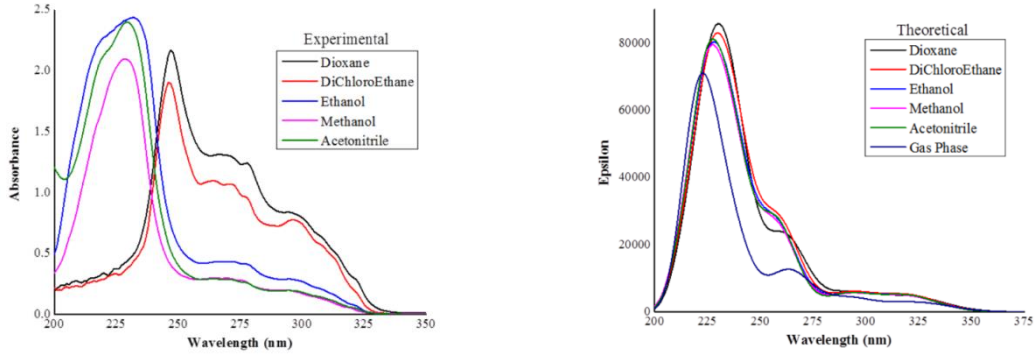

Fig. 5. Electronic absorption spectra of compound **2**, experimental in dioxane, dichloroethane, ethanol, methanol and acetonitrile, theoretical in dioxane, dichloroethane, ethanol, methanol, acetonitrile and gas phase.

Table 7

Experimental and theoretical UV spectra of compound **2**, calculated at TD-B3LYP/6-311++G(d,p).

	Experimental		Theoretical			
	$\lambda_{max, nm}$	Abs	λ_{nm}	E(eV)	f	Major contribution
Gas phase	—	—	228	5.4338	0.2674	H-2->L+2(20%), H-2->L+3(44%)
	—	—	264	4.6846	0.1206	H-3->L(24%), H-2->L(50%), H-1->L+1(26%)
	—	—	273	4.5428	0.0128	H-2->L(26%), H-1->L+1(26%), H->L+1(46%)
	—	—	294	4.2223	0.0407	H-1->L(79%)
1,4-Dioxane	247	2.17	246	5.0532	0.0256	H->L+4(31%), H->L+5(64%)
	266	1.313	262	4.7301	0.2697	H-3->L(22%), H-2->L(51%), H-1->L+1(21%)
	278	1.243	271	4.5744	0.0119	H-2->L(19%), H->L+1(37%), H->L+2(19%)
	295	0.839	294	4.2218	0.0755	H-1->L(100%)
DiChloroEthane	246	1.904	244	5.0756	0.0839	H->L+4(55%)
	264	1.097	261	4.7489	0.0356	H-1->L+1(33%), H->L+2(67%)
	271	1.07	271	4.5683	0.0022	H->L+1(14%), H->L+2(75%)
	296	0.777	293	4.2333	0.0790	H-1->L(97%)

Ethanol	232	2.439	231	5.3622	0.1433	H-4->L(55%), H-2->L+1(23%)
	266	0.434	261	4.7516	0.0268	H-1->L+1(38%), H->L+3(62%)
	277	0.414	272	4.5627	0.0019	H->L+2(81%)
	295	0.291	293	4.2377	0.0738	H-1->L(97%)
Methanol	228	2.096	227	5.4647	0.2509	H-2->L+1(17%), H-2->L+3(39%)
	264	0.298	261	4.7522	0.0247	H-1->L+1(39%), H->L+3(62%)
	275	0.281	272	4.5617	0.0019	H->L+2(81%)
	294	0.201	292	4.2391	0.0717	H-1->L(95%)
Acetonitrile	229	2.402	231	5.3650	0.1383	H-4->L(49%), H-2->L+1(20%)
	264	0.291	261	4.7521	0.0253	H-1->L+1(39%), H->L+3(61%)
	271	0.287	272	4.5613	0.0019	H->L+2(81%)
	294	0.197	293	4.2386	0.0725	H-1->L(95%)

3.7. 3. *Absorption spectra and solvent effects of compound **3**.*

Compound **3** is obtained by insertion -OCH3 group in the para position of 4-aryl of compound **1**. The experimental and theoretical electronic absorption spectra of compound **3** in 1,4-Dioxane and DiChloroEthane as non-polar solvents and Ethanol, Methanol and Acetonitrile as polar solvents are shown in (Fig. 6) and (Table 8).

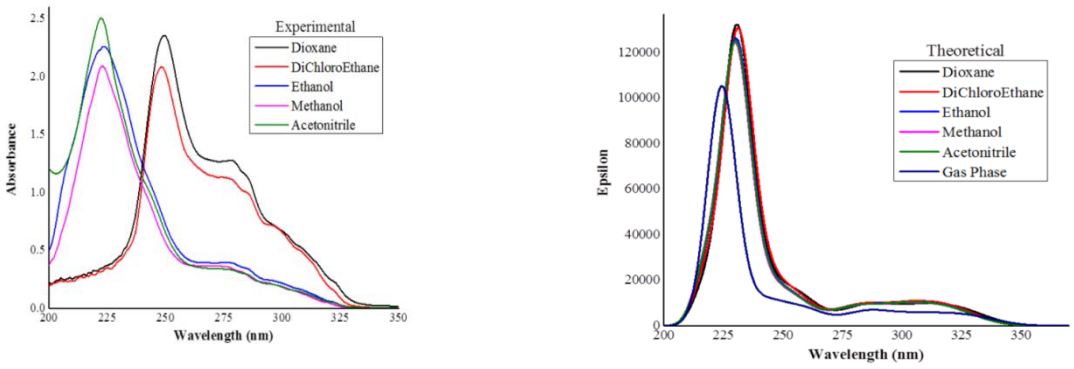

Fig. 6. Electronic absorption spectra of compound **3**, experimental in dioxane, dichloroethane, ethanol, methanol and acetonitrile, theoretical in dioxane, dichloroethane, ethanol, methanol, acetonitrile and gas phase.

Table 8 Experimental and theoretical UV spectra of compound **3**, calculated at TD-B3LYP/6-311++G(d,p).

	Experimental		Theoretical			
	$\lambda_{max, nm}$	Abs	λ_{nm}	E(eV)	f	Major contribution
Gas phase	—	—	229	5.4237	0.0391	H-2->L+3(15%), H->L+6(32%)
	—	—	275	4.5099	0.0238	H-1->L+1(34%), H->L+1(45%)
	—	—	291	4.2626	0.0311	H-2->L(40%), H-2->L+1(16%), H->L+1(21%)
1,4-Dioxane	249	2.356	248	5.0004	0.0215	H-1->L+2(21%), H->L+4(57%)
	278	1.279	273	4.5443	0.0329	H-1->L+1(41%), H->L+1(48%)
	295	0.733	291	4.2579	0.0386	H-2->L(42%), H->L+1(21%)
DiChloroEthane	248	2.085	246	5.0340	0.0965	H-1->L+2(57%), H-1->L+3(24%)
	274	1.133	271	4.5834	0.0349	H-1->L+1(51%), H->L+1(40%)

	294	0.723	291	4.2612	0.0350	H-2->L(38%), H->L+1(27%)
Ethanol	223	2.259	222	5.5845	0.0528	H-1->L+5(41%), H->L+6(23%)
	275	0.393	270	4.5925	0.0335	H-1->L+1(54%), H->L+1(37%)
	293	0.246	291	4.2629	0.0329	H-2->L(36%), H->L+1(29%)
Methanol	223	2.095	222	5.5862	0.0551	H-1->L+5(38%), H->L+6(25%)
	272	0.364	270	4.5942	0.0328	H-1->L+1(53%), H->L+1(36%)
	292	0.225	291	4.2635	0.0322	H-1->L(94%)
Acetonitrile	222	2.506	222	5.5859	0.0529	H-1->L+5(37%), H->L+6(28%)
	272	0.341	270	4.5944	0.0332	H-1->L+1(53%), H->L+1(36%)
	294	0.212	291	4.2633	0.0325	H-2->L(36%), H->L+1(29%)

The diagrams of some selected HOMO and LUMO charge density maps are indicated in (Fig. 4). In all polar and non-polar solvents compound **3** exhibited three bands, increasing solvent polarity from 1,4-Dioxane to Acetonitrile results in a blue shift (~ 27 nm) of the first band only but the other bands didn't affect by increasing solvent polarity. The first band has high intensity band in 1,4-Dioxane, DiChloroEthane, Ethanol, Methanol and Acetonitrile, but the other two bands show week and a broad bands in all solvents expect Dioxane and DiChloroEthane. All electronic absorption bands for compound **3** were listed in Table 8.

3. 7. 4 Absorption spectra and solvent effects of compound

Compound **4** results by insertion -NO_2 group in the para position of 4-aryl of compound **1**. The experimental and theoretical electronic absorption spectra of compound **4** in 1,4-Dioxane and DiChloroEthane as non-polar solvents and Ethanol, Methanol and Acetonitrile as polar solvents are shown in (Fig. 7) and (Table 9).

The charge density maps of some selected HOMO and LUMO are designated in (Fig. 4). In all polar and non-polar solvents, compound **4** exhibited three bands, increasing solvent polarity from1,4-Dioxane to Acetonitrile results in a blue shift (~ 24 nm) of the first band but the other bands didn't influence by increasing solvent polarity. The first band has high intensity in Ethanol, Methanol and Acetonitrile, although the first and second bands are broad in 1,4-Dioxane and DiChloroEthane. All electronic absorption bands for compound **4** are listed in Table 9.

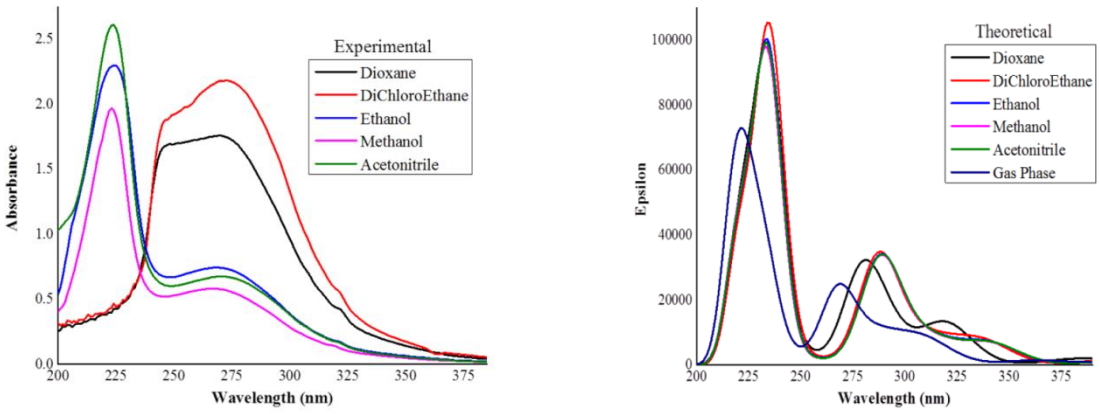

Fig. 7. Electronic absorption spectra of compound **4**, experimental in dioxane, dichloroethane, ethanol, methanol and acetonitrile, theoretical in dioxane, dichloroethane, ethanol, methanol, acetonitrile and gas phase.

Table 9
Experimental and theoretical UV spectra of compound **4**, calculated at TD-B3LYP/6-311++G(d,p).

	Experimental		Theoretical			
	$\lambda_{max, nm}$	Abs	λ_{nm}	E(eV)	f	Major contribution
Gas phase	—	—	224	5.5306	0.2701	H-2->L+2(30%), H-2->L+3(29%)
	—	—	268	4.6188	0.2781	H-4->L(93%)
	—	—	317	3.9041	0.0361	H->L+1(97%)
1,4-Dioxane	246	1.68	236	5.2547	0.7199	H->L+5(92%)
	270	1.76	279	4.4423	0.3268	H-4->L(97%)
	321	0.43	321	3.8522	0.0875	H-2->L(93%)
DiChloroEthane	246	1.877	235	5.2550	0.5703	H-1->L+4(27%), H->L+5(39%)
	273	2.182	272	4.5589	0.0132	H-5->L(95%)
	321	0.565	315	3.9364	0.0740	H->L+1(95%)
Ethanol	225	2.30	226	5.4798	0.0977	H-2->L+2(37%), H-2->L+3(49%)
	269	0.745	274	4.5227	0.0145	H-5->L(94%)
	319	0.183	314	3.9403	0.0705	H->L+1(95%)
Methanol	223	1.97	225	5.5065	0.1500	H-5->L+1(24%), H-4->L+1(26%)
	267	0.583	274	4.5168	0.0149	H-5->L(94%)
	319	0.147	315	3.9416	0.0690	H->L+1(95%)
Acetonitrile	224	2.611	225	5.5059	0.1459	H-3->L+1(22%), H-1->L+5(53%)
	270	0.677	274	4.5151	0.0148	H-5->L(94%)
	319	0.178	314	3.9411	0.0697	H->L+1(95%)

4. Conclusion

The molecular geometry of 4H-benzo[h]chromene derivatives in the ground state have been calculated by using DFT B3LYP/ 6-311++G (d,p) level of theory. The optimized structure of the studied molecules 1-4 is non-linear with the phenyl at position 4 is out of the molecular plane of the rest of the compound, the reason why no substituent effect and solvent effect were observed. The HOMO-LUMO energy gap helped in analyzing the chemical reactivity, hardness, softness, chemical potential and electro negativity. The calculated dipole moment and first order hyperpolarizability results indicate that the molecule has a reasonable good non-linear optical behaviour. The NBO analysis indicated the intermolecular charge transfer between the bonding and antibonding orbital's. Electronic spectra of 4H-benzo[h]chromene and some of its derivatives in different organic solvents such as 1,4-Dioxane and DiChloroEthane as non-polar solvents and Ethanol, Methanol and Acetonitrile as polar solvents are investigated experimentally and theoretically using the TD-DFT method at the B3LYP/6-311++G(d,p) level of the theory at the PCM model. The observed UV spectra of the studied compounds show a noticeable dependence on solvent polarity. All compounds show a blue shift (17-25 nm) upon increasing solvent polarity in the first band.

5.

6. References

[1] A. Witaicenis, L.N. Seito, A. da Silveira Chagas, L.D. de Almeida Junior, A.C. Luchini, P. Rodrigues-Orsi, S.H. Cestari, L.C. Di Stasi, Antioxidant and intestinal anti-inflammatory effects of plant-derived coumarin derivatives, Phytomedicine. 2014, 21, 240. https://doi.org/10.1016/j.phymed.2013.09.001

[2] K.H. Randive, V. Jaishree, K.S. Patil, K. Patil, Synthesis and biological evaluation of novel coumarin derivatives as antioxidant agents, Russ. J. Bioorganic Chem. 2015, 41, 324. https://doi.org/10.1134/S1068162015030085

[3] N. Arumugam, R. Raghunathan, A.I. Almansour, U. Karama, An efficient synthesis of highly functionalized novel chromeno [4, 3-b] pyrroles and indolizino [6, 7-b] indoles as potent antimicrobial and antioxidant agents, Bioorg. Med. Chem. Lett. 2012, 22, 1375. https://doi.org/10.1016/j.bmcl.2011.12.061

[4] P.W. Smith, S.L. Sollis, P.D. Howes, P.C. Cherry, I.D. Starkey, K.N. Cobley, H. Weston, J. Scicinski, A. Merritt, A. Whittington, others, Dihydropyrancarboxamides related to zanamivir: A new series of inhibitors of influenza virus sialidases. 1. Discovery, synthesis, biological activity, and structure- activity relationships of 4-guanidino-and 4-amino-4 H-pyran-6-carboxamides, J. Med. Chem. 1988, 41, 787. https://doi.org/10.1021/jm970374b

[5] A.M. Grau, L.J. Marco, Friedlander Reaction on 2-Amino-3-cyano-4H-pyrans: Synthesis of Derivatives of 4H-pyran [2, 3-b] Quinoline, New Tacrine Analogues, Bioorg. Med. Chem. Lett. 1997, 7, 3165. https://doi.org/10.1016/S0960-894X(97)10165-2

[6] J. Mori, M. Iwashima, M. Takeuchi, H. Saito, A synthetic study on antiviral and antioxidative chromene derivative, Chem. Pharm. Bull. 2006, 54, 391. https://doi.org/10.1248/cpb.54.391

[7] M.M. Khafagy, A.H.F. Abd El-Wahab, F.A. Eid, A.M. El-Agrody, Synthesis of halogen derivatives of benzo [h] chromene and benzo [a] anthracene with promising antimicrobial activities, Farm. 2002, 57, 715. https://doi.org/10.1016/S0014-827X(02)01263-6

[8] C.B. Sangani, N.M. Shah, M.P. Patel, R.G. Patel, Microwave assisted synthesis of novel 4H-chromene derivatives bearing phenoxypyrazole and their antimicrobial activity assess, J. Serbian Chem. Soc. 2012, 77, 1165 https://doi.org/10.2298/JSC120102030S

[9] S. Kumar, S. Bawa, S. Drabu, B.P. Panda, Design and synthesis of 2-chloroquinoline derivatives as non-azoles antimycotic agents, Med. Chem. Res. 2011, 20, 1340. https://doi.org/10.1007/s00044-010-9463-6

[10] B.F. Mirjalili, L. Zamani, K. Zomorodian, S. Khabnadideh, Z. Haghighijoo, Z. Malakotikhah, S.A.A. Mousavi, S. Khojasteh, Synthesis, antifungal activity and docking study of 2-amino-4H-benzochromene-3-carbonitrile derivatives, J. Mol. Struct. 2016, 1116, 102. https://doi.org/10.1016/j.molstruc.2016.03.002

[11] M. Mamaghani, K. Tabatabaeian, F. Shirini, M. Rassa, others, An expeditious regioselective synthesis of novel bioactive indole-substituted chromene derivatives via one-pot three-component reaction, Bioorg. Med. Chem. Lett. 2012, 22, 5956. https://doi.org/10.1016/j.bmcl.2012.07.059

[12] W.-J. Lu, K.J. Wicht, L. Wang, K. Imai, Z.-W. Mei, M. Kaiser, I.E.T. El Sayed, T.J. Egan, T. Inokuchi, Synthesis and antimalarial testing of neocryptolepine analogues: Addition of ester function in SAR study of 2, 11-disubstituted indolo [2, 3-b] quinolines, Eur. J. Med. Chem. 2013, 64, 498. https://doi.org/10.1016/j.ejmech.2013.03.072

[13] C.B. Sangani, J.A. Makawana, X. Zhang, S.B. Teraiya, L. Lin, H.-L. Zhu, Design, synthesis and molecular modeling of pyrazole--quinoline--pyridine hybrids as a new class of antimicrobial and anticancer agents, Eur. J. Med. Chem. 2014, 76, 549. https://doi.org/10.1016/j.ejmech.2014.01.018

[14] J.A. Makawana, C.B. Sangani, L. Lin, H.-L. Zhu, Schiff's base derivatives bearing nitroimidazole and quinoline nuclei: new class of anticancer agents and potential EGFR tyrosine kinase inhibitors, Bioorg. Med. Chem. Lett. 2014, 24, 1734. https://doi.org/10.1016/j.bmcl.2014.02.041

[15] B.V.S. Reddy, B. Divya, M. Swain, T.P. Rao, J.S. Yadav, M.V. Vardhan, A domino Knoevenagel hetero-Diels--Alder reaction for the synthesis of polycyclic chromene derivatives and evaluation of their cytotoxicity, Bioorg. Med. Chem. Lett. 2012, 22, 1995. https://doi.org/10.1016/j.bmcl.2012.01.033

[16] F. Xie, H. Zhao, L. Zhao, L. Lou, Y. Hu, Synthesis and biological evaluation of novel 2, 4, 5-substituted pyrimidine derivatives for anticancer activity, Bioorg. Med. Chem. Lett. 2009, 19, 275. https://doi.org/10.1016/j.bmcl.2008.09.067

[17] M.H. Ahagh, G. Dehghan, M. Mehdipour, R. Teimuri-Mofrad, E. Payami, N. Sheibani, M. Ghaffari, M. Asadi, Synthesis, characterization, anti-proliferative properties and DNA binding of benzochromene derivatives: increased Bax/Bcl-2 ratio and caspase-dependent apoptosis in colorectal cancer cell line, Bioorg. Chem. 2019, 93, 103329. https://doi.org/10.1016/j.bioorg.2019.103329

[18] L.M. Bedoya, M.J. Abad, E. Calonge, L.A. Saavedra, M. Gutierrez, V. V Kouznetsov, J. Alcami, P. Bermejo, Quinoline-based compounds as modulators of HIV transcription through NF-$κ$B and Sp1 inhibition, Antiviral Res. 2010, 87, 338. https://doi.org/10.1016/j.antiviral.2010.06.006

[19] D.C. Mungra, H.G. Kathrotiya, N.K. Ladani, M.P. Patel, R.G. Patel, Molecular iodine catalyzed synthesis of tetrazolo [1, 5-a]-quinoline based imidazoles as a new class of antimicrobial and antituberculosis agents, Chinese Chem. Lett. 2012, 23, 1367. https://doi.org/10.1016/j.cclet.2012.11.007

[20] N.R. Kamdar, D.D. Haveliwala, P.T. Mistry, S.K. Patel, Synthesis and evaluation of in vitro antitubercular activity and antimicrobial activity of some novel 4H-chromeno [2, 3-d] pyrimidine via 2-amino-4-phenyl-4H-chromene-3-carbonitriles, Med. Chem. Res. 2011, 20, 854. https://doi.org/10.1007/s00044-010-9399-x

[21] J.-F. Cheng, A. Ishikawa, Y. Ono, T. Arrhenius, A. Nadzan, Novel chromene derivatives as TNF-$α$ inhibitors, Bioorg. Med. Chem. Lett. 2003, 13, 3647. https://doi.org/10.1016/j.bmcl.2003.08.025

[22] M.N.S. Saudi, M.R. Gaafar, M.Z. El-Azzouni, M.A. Ibrahim, M.M. Eissa, Synthesis and evaluation of some pyrimidine analogs against toxoplasmosis, Med. Chem. Res. 2008, 17, 541. https://doi.org/10.1007/s00044-008-9097-0

[23] S.X. Cai, J. Drewe, W. Kemnitzer, Discovery of 4-aryl-4H-chromenes as potent apoptosis inducers using a cell-and caspase-based Anti-cancer Screening Apoptosis Program (ASAP): SAR studies and the identification of novel vascular disrupting agents, Anti-Cancer Agents Med. Chem. (Formerly Curr. Med. Chem. Agents). 2009, 9, 437. https://doi.org/10.2174/1871520610909040437

[24] J.-L. Wang, D. Liu, Z.-J. Zhang, S. Shan, X. Han, S.M. Srinivasula, C.M. Croce, E.S. Alnemri, Z. Huang, Structure-based discovery of an organic compound that binds Bcl-2 protein and induces apoptosis of tumor cells, Proc. Natl. Acad. Sci. 2000, 97, 7124. https://doi.org/10.1073/pnas.97.13.7124

[25] T.H. V Huynh, B. Abrahamsen, K.K. Madsen, A. Gonzalez-Franquesa, A.A. Jensen, L. Bunch, Design, synthesis and pharmacological characterization of coumarin-based fluorescent analogs of excitatory amino acid transporter subtype 1 selective inhibitors, UCPH-101 and UCPH-102, Bioorg. Med. Chem. 2012, 20, 683. https://doi.org/10.1016/j.bmc.2012.09.049

[26] K. Hiramoto, A. Nasuhara, K. Michikoshi, T. Kato, K. Kikugawa, DNA strand-breaking activity and mutagenicity of 2, 3-dihydro-3, 5-dihydroxy-6-methyl-4H-pyran-4-one (DDMP), a Maillard reaction product of glucose and glycine, Mutat. Res. Toxicol. Environ. Mutagen. 1997, 395, 47 https://doi.org/10.1016/S1383-5718(97)00141-1

[27] G. Bianchi, A. Tava, Synthesis of (2 R)-(+)-2, 3-Dihydro-2, 6-dimethyl-4 H-pyran-4-one, a Homologue of Pheromones of a Species in the Hepialidae Family, Agric. Biol. Chem. 1987, 51, 2001. https://doi.org/10.1080/00021369.1987.10868286

[28] C. Brühlmann, F. Ooms, P.-A. Carrupt, B. Testa, M. Catto, F. Leonetti, C. Altomare, A. Carotti, Coumarins derivatives as dual inhibitors of acetylcholinesterase and monoamine

oxidase, J. Med. Chem. 2001, 44, 3195. https://doi.org/10.1021/jm010894d

[29] S.R. Kesten, T.G. Heffner, S.J. Johnson, T.A. Pugsley, J.L. Wright, L.D. Wise, Design, synthesis, and evaluation of chromen-2-ones as potent and selective human dopamine D4 antagonists, J. Med. Chem. 1999, 42, 3718. https://doi.org/10.1021/jm990266k

[30] H.E.A. Ahmed, M.A.A. El-Nassag, A.H. Hassan, H.M. Mohamed, A.H. Halawa, R.M. Okasha, S. Ihmaid, S.M. Abd El-Gilil, E.S. Khattab, A.M. Fouda, others, Developing lipophilic aromatic halogenated fused systems with specific ring orientations, leading to potent anticancer analogs and targeting the c-Src Kinase enzyme, J. Mol. Struct. 2019, 1186, 212. https://doi.org/10.1016/j.molstruc.2019.03.012

[31] G.P. Ellis, Chromenes, chromanones, and chromones, John Wiley & Sons, New York, NY, 1977, 31, 11. https://doi.org/10.1002/9780470187012.ch1

[32] E.A.A. HAFEZ, M.H. ELNAGDI, A.G.A.L.I. ELAGAMEY, F.M.A.A. EL-TAWEEL, Nitriles in heterocyclic synthesis: novel synsthesis of benzo [c]-coumarin and of benzo [c] pyrano [3, 2-c] quinoline derivatives, Heterocycles (Sendai). 1987, 26, 903. https://doi.org/10.3987/r-1987-04-0903

[33] G.A. Reynolds, K.H. Drexhage, New coumarin dyes with rigidized structure for flashlamp-pumped dye lasers, Opt. Commun. 1975, 13, 222. https://doi.org/10.1016/0030-4018(75)90085-1

[34] H. Zollinger, Color chemistry: syntheses, properties, and applications of organic dyes and pigments, 3rd ed, John Wiley & Sons, VHCA, Zurich, Switzerland, 2003. https://doi.org/10.1002/anie.200385122

[35] E.R. Bissell, A.R. Mitchell, R.E. Smith, Synthesis and chemistry of 7-amino-4-(trifluoromethyl) coumarin and its amino acid and peptide derivatives, J. Org. Chem. 1980, 45, 2283. https://doi.org/10.1021/jo01300a003

[36] C. Sridevi, G. Shanthi, G. Velraj, Structural, vibrational, electronic, NMR and reactivity analyses of 2-amino-4H-chromene-3-carbonitrile (ACC) by ab initio HF and DFT calculations, Spectrochim. Acta Part A Mol. Biomol. Spectrosc. 2012, 89, 46. https://doi.org/10.1016/j.saa.2011.12.050

[37] J.T. Mague, S.K. Mohamed, M. Akkurt, S.H.H. Younes, M.R. Albayati, Crystal structure of 2-amino-4-(4-methoxyphenyl)-4H-benzo [g] chromene-3-carbonitrile, Acta Crystallogr. Sect. E Crystallogr. Commun. 2015, 71, o1017. https://doi.org/10.1107/S205698901502280X

[38] J. M. Seminario and P. Politter, Eds. Modern Density Functional Theory - A Tool for Chemistry. Elsevier, 1995, pages 1-405.

[39] W. Al Zoubi, A. A. S. Al-Hamdani, P. Widiantara, R. G. Hamoodah, Y. Gun Ko, Theoretical studies and antibacterial activity for Schiff base complexes, J. Phys. Org. Chem. 2017, 30, e3707. https://doi.org/10.1002/poc.3707

[40] V. T. Suleman, A. A. S. Al-Hamdani, S. D. Ahmed, V. Y. Jirjees, M. E. Khan, A. Dib, W. Al Zoubi, Y. Gun Ko, Phosphorus Schiff base ligand and its complexes: Experimental and theoretical investigations, Appl. Organometal. Chem. 2020, 34, e5546. https://doi.org/10.1002/aoc.5546

[41] V. Y. Jirjees, V. T. Suleman, A. A. S. Al-Hamdani, S. D. Ahmed, Preparation, Spectroscopic Characterization and Theoretical Studies of Transition Metal Complexes with 1-[(2-(1*H*-indol-3-yl)ethylimino)methyl]naphthalene-2-ol Ligand, Asian J. Chem. 2019, 31, 2430, https://doi.org/10.14233/ajchem.2019.21908

[42] A.M. El-Maghraby, Green chemistry: new synthesis of substituted chromenes and benzochromenes via three-component reaction utilizing Rochelle salt as novel green catalyst, Org. Chem. Int. 2014, 2014, 1. https://doi.org/10.1155/2014/715091

[43] R.A. Gaussian09, 1, mj frisch, gw trucks, hb schlegel, ge scuseria, ma robb, jr cheeseman, g. Scalmani, v. Barone, b. Mennucci, ga petersson et al., gaussian, Inc., Wallingford CT. 2009, 121, 150. http://gaussian.com/g09citation

[44] C. Lee, W. Yang, R.G. Parr, Development of the Colle-Salvetti correlation-energy formula into a functional of the electron density, Phys. Rev, 1988, Vol. B. 37, 785. https://doi.org/10.1103/PhysRevB.37.785

[45] A.D. Becke, Density-functional thermochemistry. III. The role of exact exchange, J. Chem. Phys. 1993, 98, 5648. https://doi.org/10.1063/1.464913

[46] R.G. Parr, W. Yang, Density-functional theory of atoms and molecules Oxford Univ. Press, New York, 1989 https://doi.org/10.1002/qua.560470107

[47] M.J. Frisch, G.W. Trucks, H.B. Schlegel, G.E. Scuseria, M.A. Robb, J.R. Cheeseman, G. Scalmani, V. Barone, G.A. Petersson, H. Nakatsuji, others, Gaussian 16, (2016).

[48] T. Koopmans, The classification of wave functions and eigen-values to the single electrons of an atom, Physica. 1934, 1, 104. https://doi.org/10.1016/S0031-8914(34)90011-2

[49] J.C. Phillips, Generalized Koopmans' Theorem, Phys. Rev. 1961, 123, 420. https://doi.org/10.1103/PhysRev.123.420

[50] F. Weinhold, C.R. Landis, E.D. Glendening, What is NBO analysis and how is it useful?, Int. Rev. Phys. Chem. 2016, 35, 399 https://doi.org/10.1080/0144235X.2016.1192262

[51] A.E. Reed, L.A. Curtiss, F. Weinhold, Intermolecular interactions from a natural bond orbital, donor-acceptor viewpoint, Chem. Rev. 1988, 88, 899. https://doi.org/10.1021/cr00088a005

[52] C.M. Rohlfing, L.C. Allen, R. Ditchfield, Proton and carbon-13 chemical shifts: comparison between theory and experiment, Chem. Phys. 1984, 87, 9. https://doi.org/10.1016/0301-0104(84)85133-2

[53] K. Wolinski, J.F. Hinton, P. Pulay, Efficient implementation of the gauge-independent atomic orbital method for NMR chemical shift calculations, J. Am. Chem. Soc. 1990, 112, 8251. https://doi.org/10.1021/ja00179a005

[54] S. Murugavel, P.S. Kannan, A. SubbiahPandi, T. Surendiran, S. Balasubramanian, 2, 3, 4, 9-Tetrahydro-1H-carbazole, Acta Crystallogr. Sect. E Struct. Reports Online. 2008, 64, o2433. https://doi.org/10.1107/S1600536808038713

[55] F. Jensen, Introduction to computational chemistry, John wiley & sons, 2017, (Chapter 9), p. 309, p. 492, (Chapter 6), p. 257.

[56] C. Morell, A. Grand, A. Toro-Labbe, New dual descriptor for chemical reactivity, J. Phys. Chem. A. 2005, 109, 205. https://doi.org/10.1021/jp046577a

[57] C.C. Ersanli, G.K. Kantar, S. \cSa\csmaz, Crystallographic, spectroscopic (FTIR and NMR) and quantum computational calculation studies on bis (2-methoxy-4-((E)-prop-1-enyl) phenyl) oxalate, J. Mol. Struct. 2017, 1143, 318. https://doi.org/10.1016/j.molstruc.2017.04.032

[58] F. Weinhold, C.R. Landis, Natural bond orbitals and extensions of localized bonding concepts, Chem. Educ. Res. Pract. 2001, 2, 91. https://doi.org/10.1039/B1RP90011K

[59] S. Natarajan, G. Shanmugam, S.A. Martin Britto Dhas, Growth and characterization of a new semi organic NLO material: L-tyrosine hydrochloride, Cryst. Res. Technol. J. Exp. Ind. Crystallogr. 2008, 43, 561. https://doi.org/10.1002/crat.200711048

[60] J. Zyss, D.S. Chemla, Quadratic nonlinear optics and optimization of second-order nonlinear response of organic molecules and crystals, Nonlinear Opt. Prop. Org. Mol. Cryst. 1987, 1, 23. https://doi.org/10.1016/B978-0-12-170611-1.50006-1

[61] D.S. Bradshow, D.L. Andrews, Quantum channels in nonlinear optica l processes, J Nonlinear Opt Phys Matter. 2009, 18, 285. https://doi.org/10.1142/S0218863509004609

[62] J.P. Abraham, D. Sajan, I.H. Joe, V.S. Jayakumar, Molecular structure, spectroscopic studies and first-order molecular hyperpolarizabilities of p-amino acetanilide, Spectrochim. Acta Part A Mol. Biomol. Spectrosc. 2008, 71, 355. https://doi.org/10.1016/j.saa.2008.01.010

[63] P. Karamanis, C. Pouchan, G. Maroulis, Structure, stability, dipole polarizability and differential polarizability in small gallium arsenide clusters from all-electron ab initio and density-functional-theory calculations, Phys. Rev. A. 2008, 77, 013201. https://doi.org/10.1103/PhysRevA.77.013201

[64] A. Ben Ahmed, H. Feki, Y. Abid, H. Boughzala, A. Mlayah, Structural, vibrational and theoretical studies of l-histidine bromide, J. Mol. Struct. 2008, 888, 180. https://doi.org/10.1016/j.molstruc.2007.11.056

[65] H. Alyar, Z. Kantarci, M. Bahat, E. Kasap, Investigation of torsional barriers and nonlinear optical (NLO) properties of phenyltriazines, J. Mol. Struct. 2007, 834, 516. https://doi.org/10.1016/j.molstruc.2006.11.066

[66] C. Adant, M. Dupuis, J.L. Bredas, Ab initio study of the nonlinear optical properties of urea: electron correlation and dispersion effects, Int. J. Quantum Chem. 1995, 56, 497. https://doi.org/10.1002/qua.560560853

[67] L. Sun Pu, Observing High Second Harmonic Generation and Control of Molecular Alignment in One Dimension, 1991. https://doi.org/10.1021/bk-1991-0455.ch022.